

NUMERICAL EVALUATION OF THE CONTRIBUTION OF THE STICK MODEL-INDUCED ELASTIC STREAMWISE CAMBER DEFORMATION TO THE FLUTTER SPEED OF A SWEEP WING

Paper No. 2004-23, Presented at the MSC.Software Virtual Product Development Conference, Huntington Beach, California, October 18-20, 2004

by

Emil Suciu* and Jose Luis Panza**

ABSTRACT

When the aerodynamic derivatives factoring method is used with the DLM, the elastic streamwise camber deformation at the aerodynamic surface is automatically separated from other types of motion. For a highly swept wing with structure modeled as a swept beam, the difference in the flutter speed calculated with/without streamwise camber terms included in the generalized aerodynamics can be large.

*Precision Conversions, Escondido, California 92025, esuciu@yahoo.com

**Structural Analysis Group Manager, General Atomic Aeronautical Systems Inc., Rancho Bernardo, CA 92127, panzaj@gat.com

1.0 Introduction

Throughout this paper, “**elastic streamwise camber deformation**” will be used interchangeably with “**dynamic camber**” or with “**dynamic camber deformation**”. The terms “**stick model**” or “**beam model**” are also interchangeable.

The stick model has enjoyed a long and successful period of use with applications to flutter and dynamic analyses for aircraft of all types and sizes and categories, except perhaps delta-winged aircraft.

It is well known that for any swept or unswept lifting surface structure, elastic streamwise camber deformation occurs in the structure for some or for all of the elastic modes of vibration.

It is also known that unswept or swept stick models do not contain sufficient structural detail to analytically represent the actual structural dynamic camber deformation of lifting surfaces; further, the actual structural dynamic camber deformation cannot be imparted to the aerodynamic surface by either a swept or by an unswept stick model.

It will be shown here that the swept stick model induces an artificial dynamic camber at the aerodynamic surface. The effect which this artificial elastic streamwise camber deformation at the aerodynamic surface has on the calculated flutter speed of a swept wing with structure modeled as a swept beam will be isolated and quantified.

The analysis program is the MSC.Nastran Aeroelastic Analysis Package with the Doublet Lattice Method (DLM) as the unsteady aerodynamics method (Reference 1).

Motion transfer from the stick model to the aerodynamic surface is through the use of beam splines with rigid arms (the SPLINE2 card, Reference 1) for all the cases discussed. An equivalent way of stating this is that linear extrapolations of the motions from the beam to the aerodynamic points in planes normal to the elastic axis are performed. The mathematical details of the extrapolation process can be found in Reference 1.

If the stick model has zero sweep angle, there is no elastic streamwise camber deformation (dynamic camber) arising at the aerodynamic surface for any mode of vibration. If the sweep angle of the stick model is

different from zero, an artificial dynamic camber deformation at the aerodynamic surface appears and varies with the sweep angle in some fashion for any elastic mode, bending or torsion. The artificial dynamic camber is dependent on the mode shape. See Figure 1 where it can be seen that the motions at the center of each box of a streamwise aerodynamic strip are imparted from a different point of the beam elastic axis idealization than for any other box.

For a swept lifting surface, as for an unswept one, there is no structural detail between the elastic axis structural idealization and the leading and trailing edges of the wing to define any kind of dynamic camber deformation anywhere. See again Figure 1. The structural motion defined at the beam is linearly extrapolated to the aerodynamic surface, with the perils associated with extrapolation of any kind, even though the results of linear extrapolation are not as dramatic as the results from other types of extrapolation; see for example the cubic or surface splines rambling outside the region of constraint (the potato chip effect). For this reason, the dynamic camber deformation which arises at the aerodynamic surface as a result of using a swept beam model is considered to be artificial.

When the aerodynamic derivatives factoring method (Reference 2) is used with the DLM, the elastic mode shapes at every aerodynamic box are automatically descrambled into simpler and always the same motions: heave, streamwise torsion, control surface rotation, tab rotation and elastic streamwise camber deformation. The unsteady aerodynamic forces and moments arising from the dynamic camber deformation of a lifting surface are automatically separated from the unsteady forces and moments resulting from the other types of motion and the effect of keeping or discarding the camber deformation terms in the generalized aerodynamics can be studied with ease.

2.0 Flutter Analysis of a Swept Wing with the Structure Idealized as a Swept Beam and Using the SPLINE2 Card for Motion Transfer from Structure to the Aerodynamic Surface.

The wing and the fuselage are present in the structural dynamic analysis, but the fuselage is not modeled aerodynamically. Figure 1 shows the swept wing configuration analyzed. A typical wing strip with the DLM aerodynamic box arrangement is shown. Structural displacements are enforced from the swept elastic axis to the centers of the aerodynamic boxes using the SPLINE2 card. It can be seen from Figure 1 that each aerodynamic box on the strip receives its motion from a different point on the elastic axis than any other box.

Figure 2 shows the modal deformation vs. the undeformed shape for the wing second torsional mode.

The DLM and the aerodynamic derivatives factoring method with its motion descrambling capability are used with all aerodynamic factors being equal to 1.000. Figures 3.a and 3.b show the total interpolated motion at the aerodynamic strip pictured in Figure 1 (the 12th spanwise strip for the wing), along with the descrambled motions for the wing second torsional mode: bending, streamwise torsion and artificial elastic streamwise camber deformation.

The descrambled and the total real and imaginary chordwise pressure distributions for the wing second torsional mode at the aerodynamic strip of Figure 1 for a k-value of 0.35 are shown in Figures 4.a and 4.b.

The descrambled and total real and imaginary spanwise lift distributions and spanwise moments distributions about the wing leading edge can be seen in Figures 5.a and 5.b and Figures 6.a and 6.b respectively for the wing second torsional mode for the k-value of 0.35.

Figures 4.a through 6.b clearly illustrate the complete control afforded the user by the aerodynamic derivatives factoring method over all the aerodynamic forces and moments acting on a lifting surface moving in a general mode of vibration.

The K-E method is used for the symmetric free-free flutter analyses of the wing.

The flutter mechanism is wing first bending with wing first torsion with the wing second vertical bending and the wing second torsion also participating in the flutter mechanism.

First, a flutter analysis is performed with the artificial dynamic camber deformation terms for all modes included in the generalized aerodynamics and the V-g plot for this wing is shown in Figure 7 for a given altitude and Mach Number. The calculated flutter speed is 672 KEAS.

Second, the flutter analysis is performed with the artificial dynamic camber deformation forces and moments removed from the generalized aerodynamic forces matrices QHHL for all modes. The V-g plot is shown in Figure 8, for the same altitude and Mach Number as for the previous analysis. The calculated flutter speed with camber

deformation removed is 624 KEAS. The difference in flutter speed from the previous case is $\Delta V_c = 48$ KEAS, which is the contribution of the stick model-induced artificial elastic streamwise camber deformation. Flutter speed changes of this magnitude can usually be seen after the application of large factors on some aerodynamic parameters.

The V-f plots corresponding to the V-g plots of Figures 7 and 8 are shown in Figures 9 and 10 respectively. The torsional frequency at flutter is 6.1 Hz for the case when camber deformation is included and 5.9 Hz for the case without artificial camber deformation. The change in frequency is not as large percentagewise as the airspeed change.

The results presented in this paper were obtained with the use of computer program LSP3 (Lifting Surface Program 3) which implements the aerodynamic derivatives factoring method through automatic descrambling of the modal motion and the calculation of the associated descrambled forces and moments which are then available for factoring.

The calculation of the contribution of the artificial dynamic camber ΔV_c (but without mode shapes descrambling and calculation of the descrambled forces and moments) can also be achieved without the use of program LSP3 simply by placing streamwise RBARs from the elastic axis grid points to corresponding grid points defined on the leading and trailing edges of the lifting surface at the same spanwise station to force their motion and then using surface splines (the SPLINE1 card) constrained by the elastic axis grid points and the leading and trailing edge points to transfer the motion from the structure to the aerodynamic surface. Within the numerical accuracy of the surface splining process, the artificial elastic streamwise camber deformation will be eliminated in this way and its contribution ΔV_c to the flutter speed of swept lifting surfaces can be obtained.

3.0 Conclusions

It has been shown numerically that the contribution ΔV_c of the stick model-induced artificial dynamic camber deformation to the flutter speed of a swept wing can be large. The calculated contribution ΔV_c is configuration-dependent and it can be either positive or negative.

For a complete aircraft modeled structurally with swept beams, even in the absence of a large database of cases to support the assertion, it is stated here that the artificial dynamic camber is responsible for contributions of anywhere between $\Delta V_c = \pm 10$ KEAS to $\Delta V_c = \pm 50$ KEAS to the calculated flutter speed of each swept lifting surface.

Static aeroelastic analyses will also have a contribution from the artificial elastic streamwise camber deformation at the aerodynamic surface arising from the use of a swept stick model.

It is suggested that flutter analyses of a swept wing represented as a stick model and then as a full finite element model (correlated to the same baseline data as the stick model) be performed in order to compare and to quantify the actual and the artificial dynamic camber deformation effects with the aid of the aerodynamic derivatives factoring method.

Experimental aerodynamic forces resulting from arbitrary elastic modes dynamic camber deformation are not likely to be available any time soon, so obviously correcting the DLM-calculated forces due to the actual structural dynamic camber with anything other than unit factors is just automatic and unintended guesswork. Factoring the aerodynamic forces due to the artificial dynamic camber is even more in the category of guesswork. This raises another question about the use of factoring methods which do not separate dynamic camber deformation from the other structural displacements.

4.0 References

1. Rodden, W.P., and Johnson, E.H., "User's Guide V.68, MSC.Nastran Aeroelastic Analysis", The MacNeal-Schwendler Corporation, Los Angeles, CA, 1994.
2. Suciu, E., Glaser, J., and Coll, R., "Aerodynamic Derivatives Factoring Scheme for the MSC.Nastran Doublet Lattice Program Including Elastic Streamwise Camber Deformation", Presented at the MSC.Nastran World Users' Conference, Los Angeles, California, March 26-30, 1990.

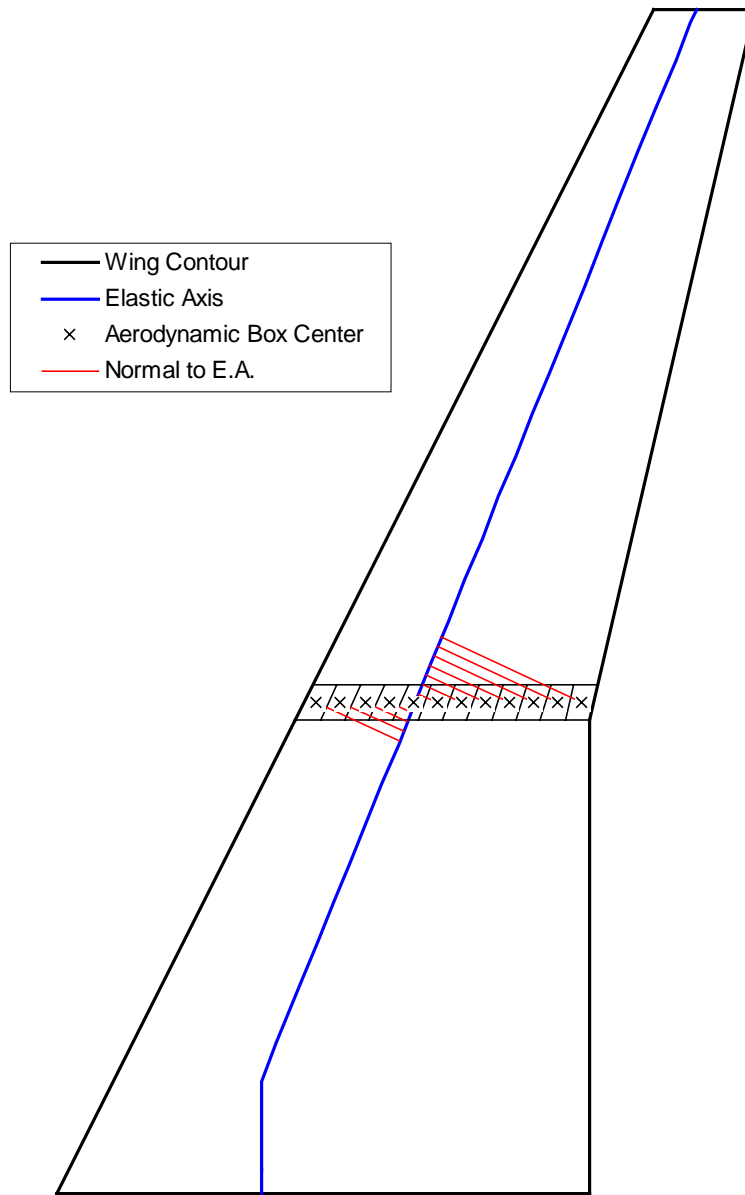


Figure 1. Swept Wing Planform With Aerodynamic Box Centers for Typical Strip. Structural Displacements are Enforced from the Swept Elastic Axis to the Aerodynamic Boxes Using the SPLINE2 Card.

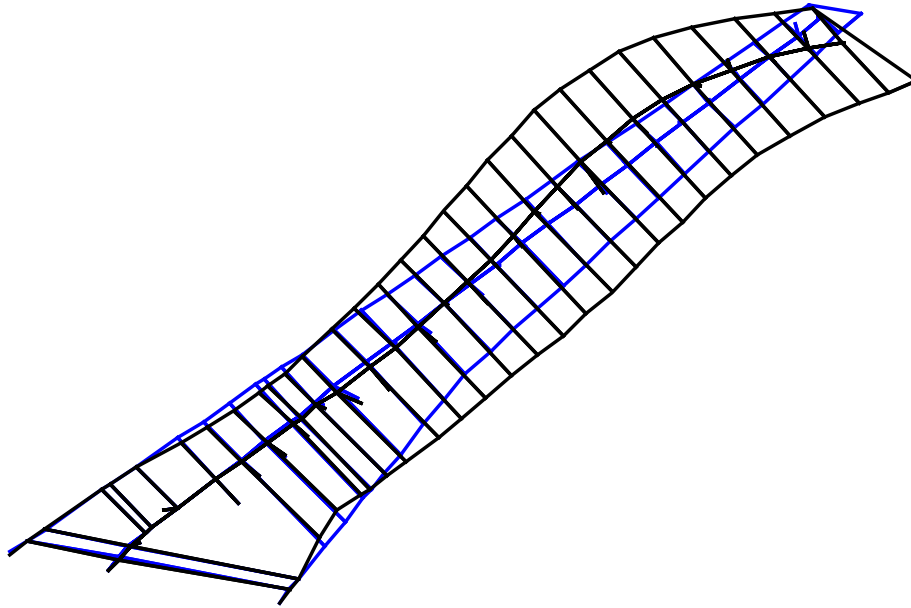


Figure 2. Wing Second Torsional Mode; Transverse Lines Are Normal to the Elastic Axis.

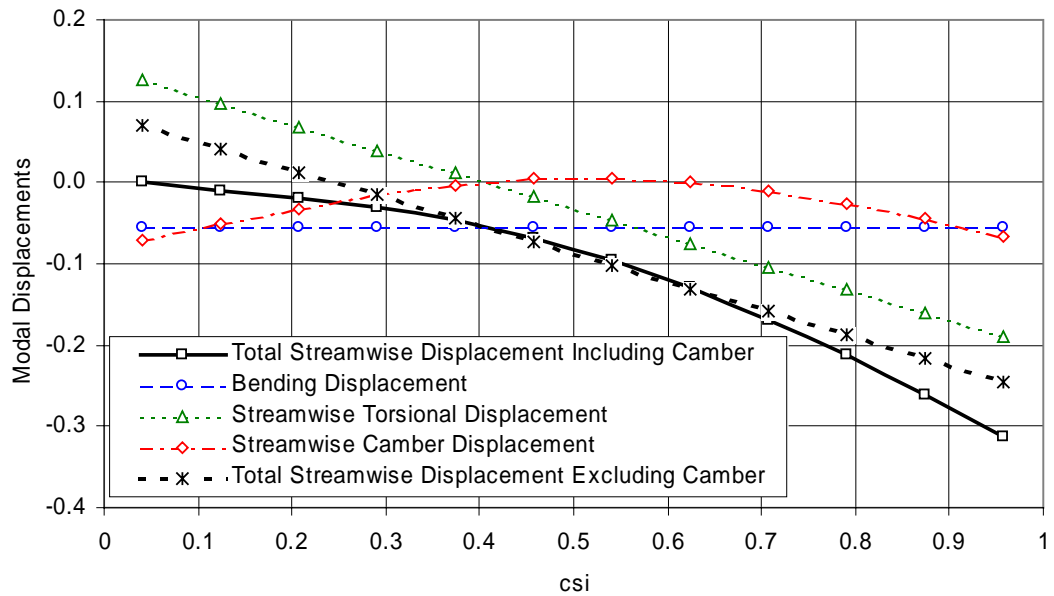


Figure 3a. Descrambled and Total Streamwise Modal Displacements at Centers of Aerodynamic Boxes of Wing Strip Shown in Figure 1 (Spanwise Strip No. 12) for the Second Wing Torsional Mode.

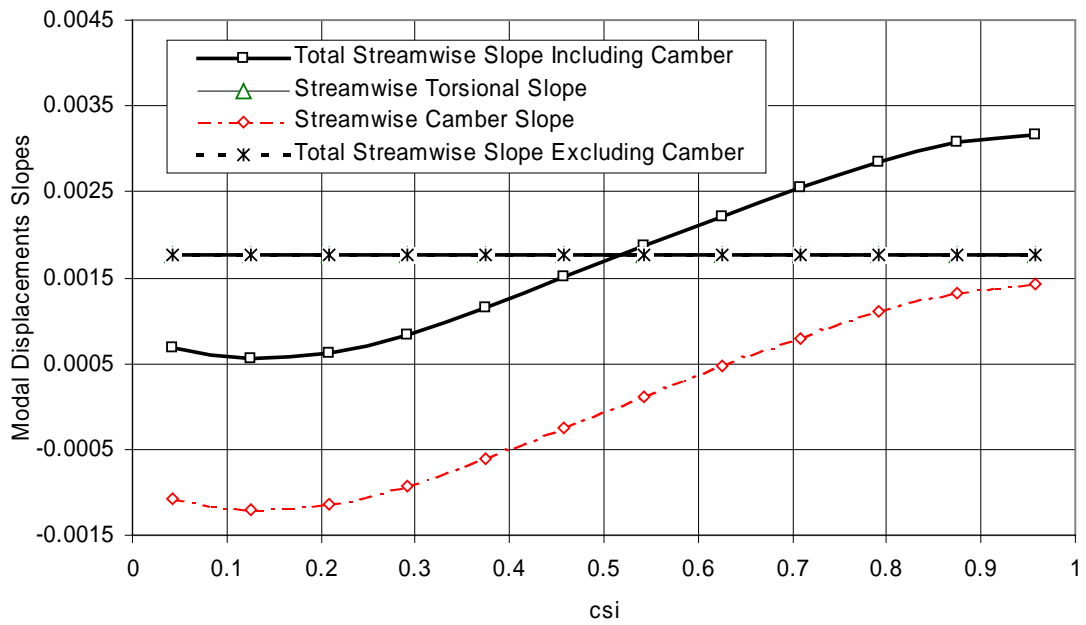


Figure 3b. Descrambled and Total Streamwise Slopes of Modal Displacements at Centers of Aerodynamic Boxes of Wing Strip Shown in Figure 1 (Spanwise Strip No. 12) for the Second Wing Torsional Mode.

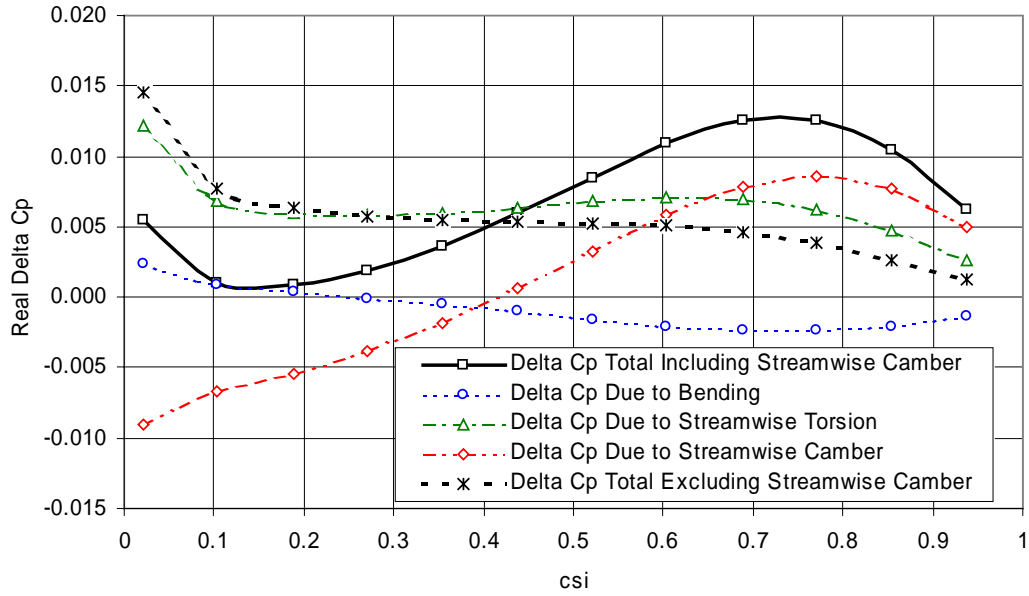


Figure 4.a. Descrambled and Total Real Chordwise Pressures at Box $\frac{1}{4}$ Chord for Wing Second Torsional Mode for Aerodynamic Strip of Figure 1 (Spanwise Strip No. 12); $k=0.35$

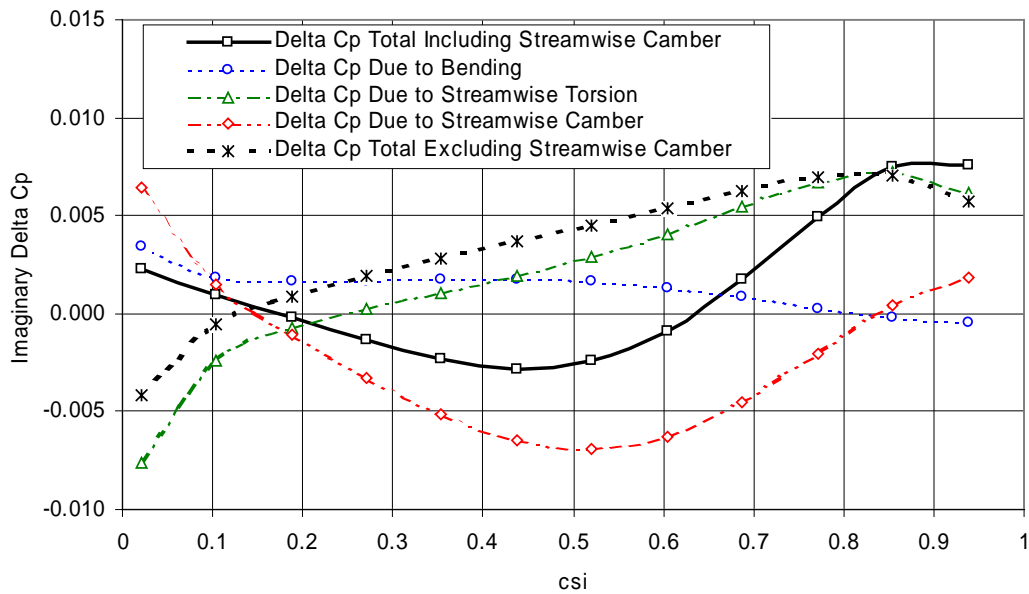


Figure 4.b. Descrambled and Total Imaginary Chordwise Pressures at Box $\frac{1}{4}$ Chord for Wing Second Torsional Mode for Aerodynamic Strip of Figure 1 (Spanwise Strip No. 12); $k=0.35$

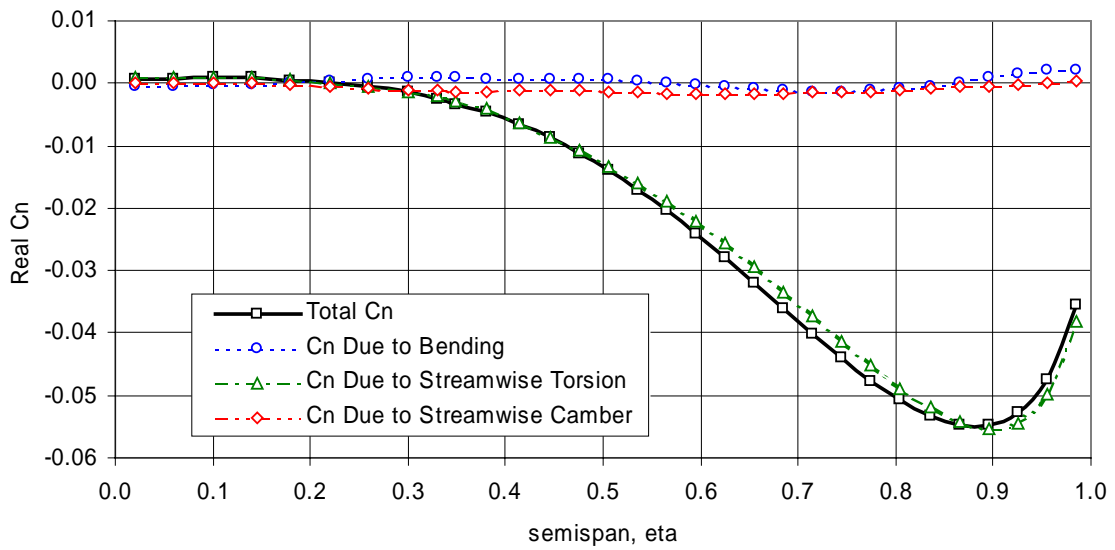


Figure 5.a. Descrambled and Total Real Spanwise Cn Distributions for Second Torsional Mode for Wing of Figure 1; $k=0.35$

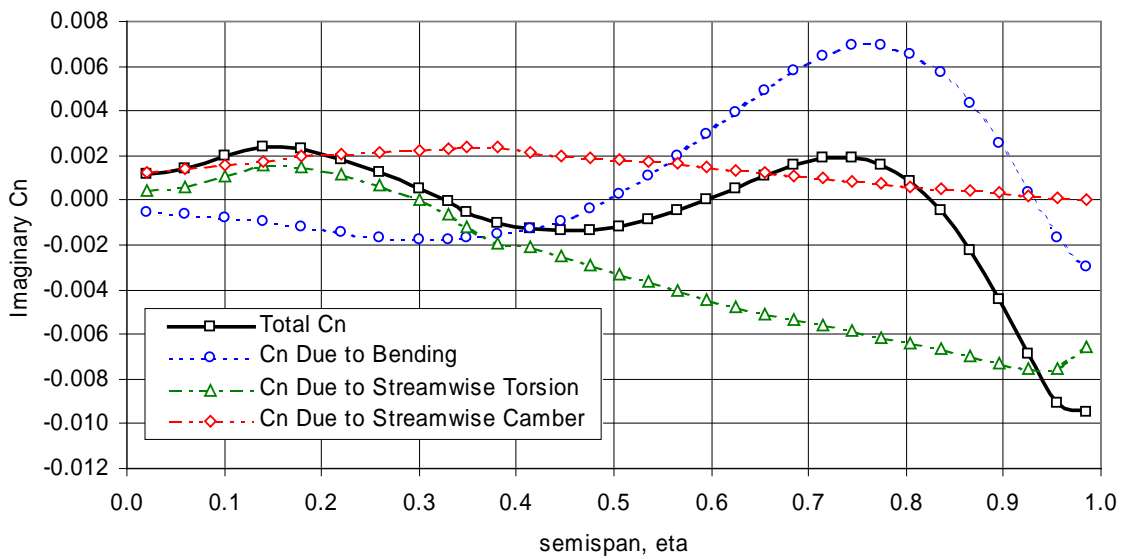


Figure 5.b. Descrambled and Total Imaginary Spanwise Cn Distributions for Second Torsional Mode for Wing of Figure 1; $k=0.35$

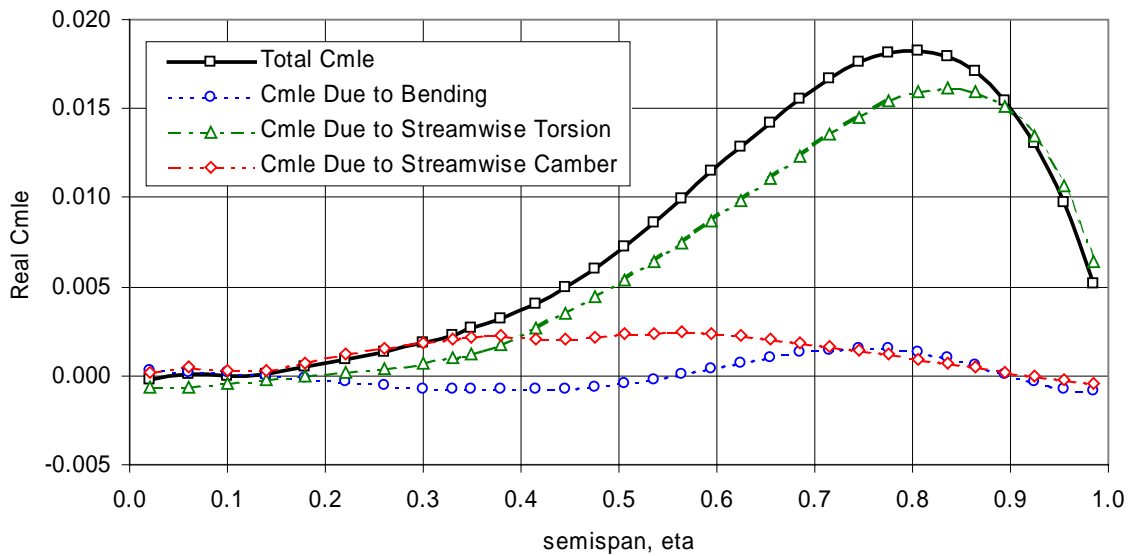


Figure 6.a. Descrambled and Total Real Spanwise Moment Distributions About the Leading Edge for Second Torsional Mode for Wing of Figure 1; $k=0.35$

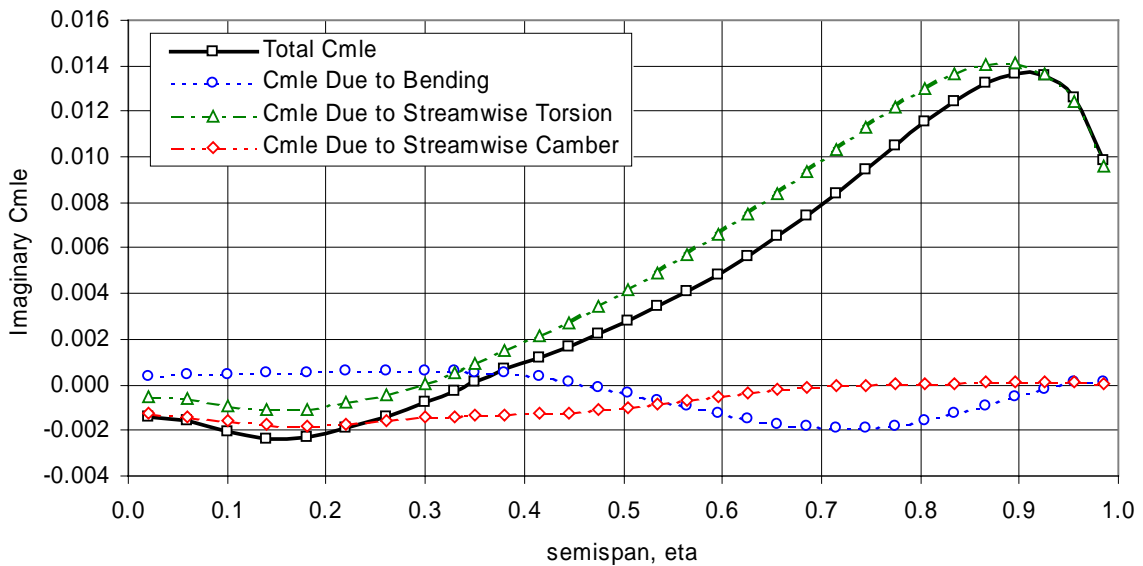


Figure 6.b. Descrambled and Total Imaginary Spanwise Moment Distributions About the Leading Edge for Second Torsional Mode for Wing of Figure 1; $k=0.35$

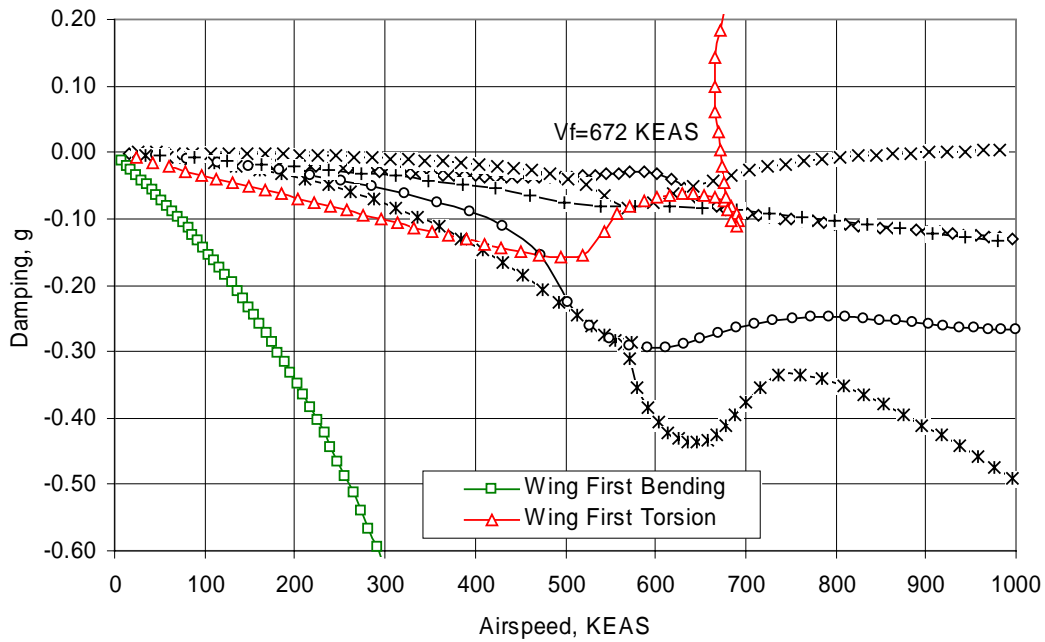


Figure 7. V-g Plot for Symmetric Flutter Analysis of Swept Wing of Figure 1; Camber Deformation Terms Are Included in the Generalized Aerodynamics Matrix.

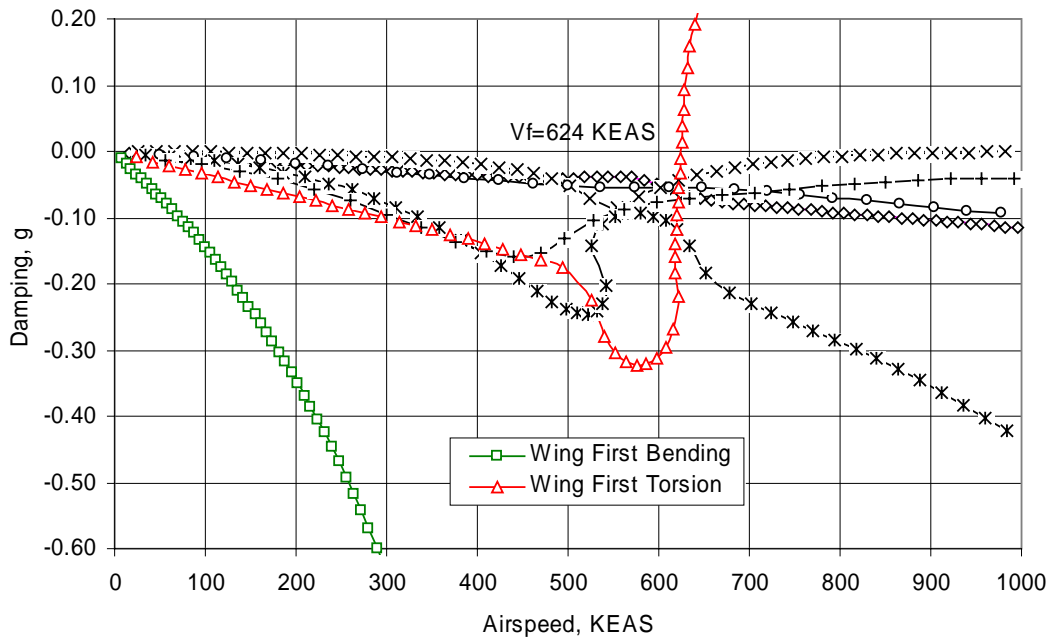


Figure 8. V-g Plot for Symmetric Flutter Analysis of Swept Wing of Figure 1; Camber Deformation Terms Have Been Removed from the Generalized Aerodynamics Matrix

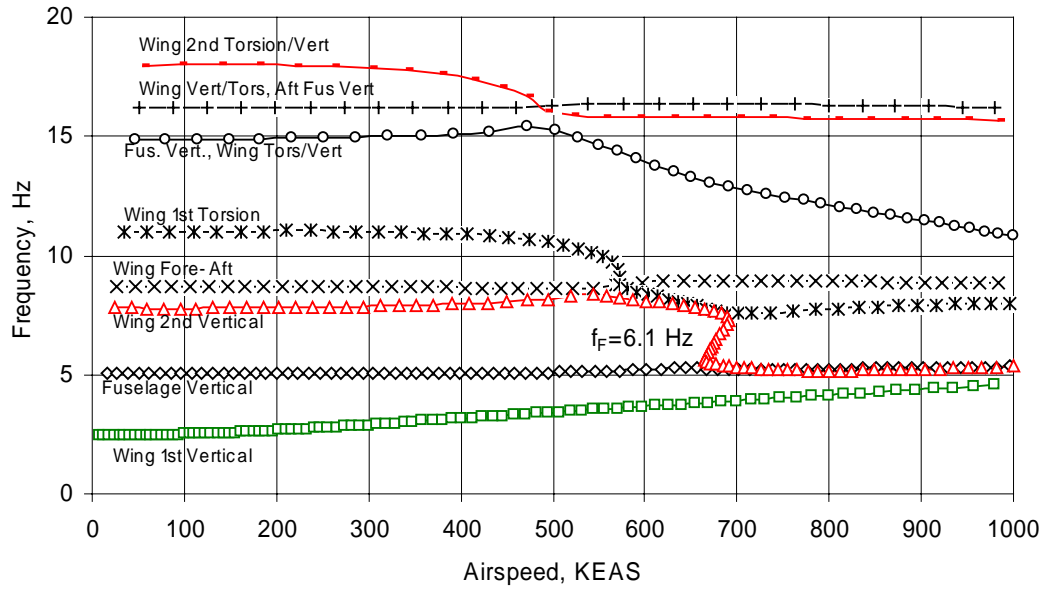


Figure 9. V-f Plot for Symmetric Flutter Analysis of Swept Wing of Figure 1; Camber Deformation Terms Are Included in the Generalized Aerodynamics Matrix.

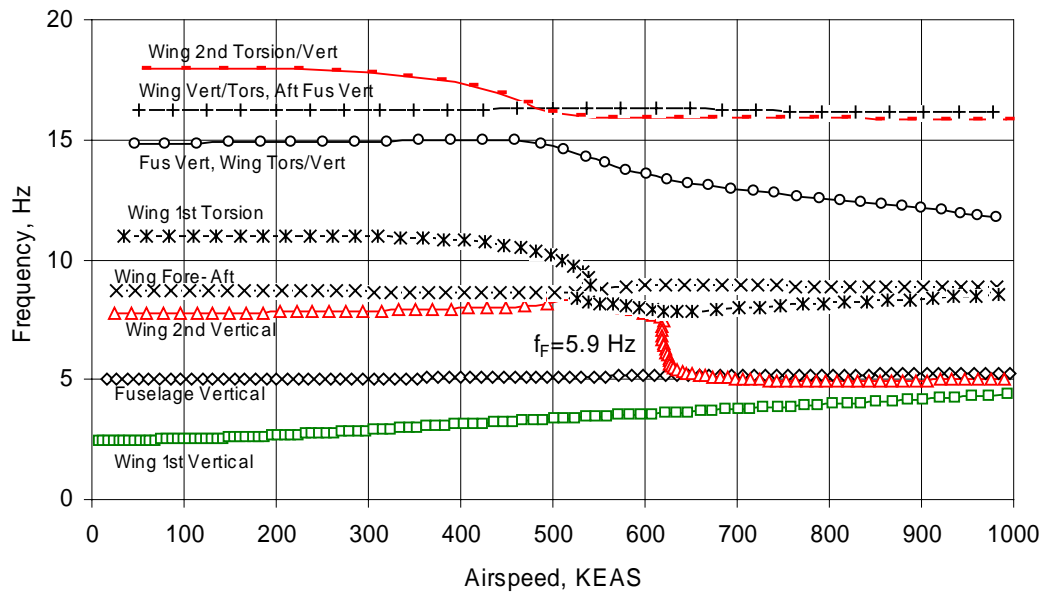


Figure 10. V-f Plot for Symmetric Flutter Analysis of Swept Wing of Figure 1; Camber Deformation Terms Have Been Removed from the Generalized Aerodynamics Matrix.